Geomechanics and Engineering, *Vol. 26, No. 1 (2021) 49-61*
https://doi.org/10.12989/gae.2021.26.1.049

Research on theory, simulation and measurement of stress behavior under regenerated roof condition

Xuelong Li[1,2,3,4], Shaojie Chen*[1,3], Qiming Zhang[2], Xin Gao[1] and Fan Feng[1]

[1]*State Key Laboratory of Mining Disaster Prevention and Control, Shandong University of Science and Technology, Qingdao, 266590, Shandong, China*
[2]*State Key Laboratory of Coal Resources and Safe Mining, China University of Mining and Technology, Xuzhou, 221116, Jiangsu, China*
[3]*College of Energy and Mining Engineering, Shandong University of Science and Technology, Qingdao, 266590, Shandong, China*
[4]*State Key Laboratory of Coal Mine Disaster Dynamics and Control, College of Resource and Safety Engineering, Chongqing University, Chongqing 400030, China*

(Received March 20, 2021, Revised June 18, 2021, Accepted June 21, 2021)

Abstract. To determine ground stress behavior under the special condition of a regenerated roof, we established a model of elastic rectangular cantilever thin plates. Moreover, the critical conditions for bending and fracturing the regenerated roof during mining were analysed. Meanwhile, by applying continua FLAC-3D numerical simulation, this research simulated changes in the stress and strain on a regenerated roof during mining and proposed prevention and control methods for dynamic disasters. The results show that: (1) the thinner the regenerated roof, the larger the tensile stress on the roof based on analysis using the theoretical model. Furthermore, the longer the advance distance during mining, the greater the tensile stress on the regenerated roof. (2) By analysing simulation results, during the fracturing of the regenerated roof, roof displacement firstly suddenly increases and then gradually decreases to be stable. Floor-heave-induced displacement presents a divergent state, that is, increases outwards in an elliptical manner. (3) For control of the regenerated roof, monitoring on activities of the roof should be strengthened and stress should be relieved timeously. Moreover, effective support methods should be taken to prevent development of hazards on working faces and roadways caused by the widespread behavior of the roof.

Keywords: elastic rectangular cantilever thin plate; ground stress behavior; numerical simulation; regenerated roof; roof control

1. Introduction

A regenerated roof refers to the roof of a lower slice re-compacted and bonded for a certain period under stratal stress due to rock bondability and addition of water and binders after roof caving of the upper slice during mining. When slicing is carried out, as part of mining operations, under a regenerated roof, due to influences of geological structure, tectonic stresses are large, so is the range of damage to coal seams, and the lower slice tends to show stress concentration (Zou *et al.* 2015, Zhang *et al.* 2021a). Meanwhile, weakly cemented masses forming the roof have a low strength and many fissures, so that accidents, such as caving of the regenerated roof readily occur, thus seriously affecting mine production safety. In addition, because of non-ideal conditions of the regenerated roof, the mining of the lower slice can severely damage overlying strata and the surface deformation can be large. Furthermore, surface subsidence occurs repeatedly when mining into deep areas, so that these, including surface buildings, railways and water bodies are severely damaged, which adversely affects the environment in mining areas (Li *et al.* 2020, Zou *et al.* 2021). Therefore, it is of significance for the safety and productivity of mines to build a theoretical mechanical model of the conditions under a regenerated roof to simulate and research instability processes and mine stress distributions.

To solve safety problems caused by the regenerated roof, some scholars have conducted experiments and research in areas, such as structural form, movement and roof control methods, etc. After analysing the ground stress behavior of a steeply inclined top-coal caving face in Huating coal mine, Gansu Province, China, Zhang *et al.* (2016) investigated the flow and caving characteristics of top coal and roof rock, as well as top coal loss pattern in the fully mechanized top coal caving mining of extra thick coal seams. Latifi *et al.* (2016) posited that composite rock beams allow movement of the roof of a working face. Combining the key strata with other strata to form a unified rock beam and determining the discriminate criterion is widely applied when mining coal seams with high gas contents. Moreover, the theory of composite rock beams provides a new idea for studying mine stress distributions. Based on similar material simulation, numerical simulation, and field measurement, Alehossein and Poulsen (2010) developed a yield and caveability criterion based on in situ conditions in the top coal in advance of the mining face (yield) and behind the supports (caveability). Based on the strain energy balance in longwall coal mining is developed to determine the mining-induced stress over gates and

*Corresponding author, Professor
E-mail: chensj@sdust.edu.cn

ISSN: 2005-307X (Print), 2092-6219 (Online)

pillars. In the proposed model, the height of the destressed zone above the mined panel, total induced stress, abutment angle, vertical component of induced stress, and coefficient of stress concentration over gates and pillars are determined analytically (Rezaei *et al.* 2015, Liu *et al.* 2021).

After observations of numerous roadway stability cases behind longwall faces, Wilson *et al.* (1983) stated that the vertical stress in the goaf increases linearly from zero to the original overburden stress at some point within the goaf. Wang *et al.* (2013) studied the stress evolution characteristics of coal pillars on a working face in the upper slice during slicing. When the width of these coal pillars varies, roof stress characteristics of the working face in the lower slice also vary. A reasonable width of coal pillar not only improves resource recovery, but also ensures safe mining of the working face in the lower slice. The permeability distribution certainly will be non-uniform and changing in the lower slice as the floor of the top slice. First, when the upper slice face is mining, the stress re-distributions lead to stress concentration in the lower slice in front of the face. Then, the floor is exposed to the goaf, and stress is relieved. Leśniak *et al.* (2020) presented the results of applying the collapsing method in mining seismology using a cloud of located events recorded during mining activity at one of the coalfaces in the Bobrek hard coal mine. Through theoretical analysis and simulation testing, Cheng *et al.* (2009) revealed mechanical equations and criteria for fracturing different roof structures and analysed the relationship between the range of influence of mining-induced stress and advancing length of the working face. Varela *et al.* (2021) evaluated the best combination of three different modular extensive green roof structures and two types of local substrates (compost and soil + biochar) for Lactuca sativa L. var. crispa (lettuce) gowth. The breaking angle and the shearing angle of the overburden strata can reflect the compaction characteristics in the floor within the goaf (Smart and Whittaker 1987, Li *et al.* 2021). Based on many site investigations, collection of field data, and by using numerical simulation and similar simulation methods, Deng *et al.* (2016) studied coal slicing and mainly focused on fracturing of overlying strata of a roof during slicing. and found that the height of the caving zone of a roof in slicing increases with the number of slices. By employing methods, such as numerical simulation, electromagnetic geophysical prospecting, and seismic monitoring, Choi and Lee (2015) used PFC-3D numerical analysis of the optimum cutter spacing and failure aspects of Korean Busan tuff, and found that PFC-3D can easily represent macroscopic rock specimens containing micro cracks.

Based on the special geological conditions prevailing at Xinji No. 2 coal mine, Huainan city, Anhui Province, China, by theoretical analysis and numerical simulation, we assessed the movement of coal and rock strata and the distribution characteristics of overlying strata in backstoping under a regenerated roof. The research also analysed the evolution and distribution of stress fields in stope based on movement of coal and rock strata and found the ways to prevent roof caving and surface damage. In addition, a method of roof control was proposed to achieve the goal of reducing and controlling the influences of backstoping as far as possible on mine safety under a regenerated roof. This not only enriches theories of ground stress behavior and movement of coal and rock strata, which supplements theoretical predictions of subsidence when mining (Singh *et al.* 2002, Zhang *et al.* 2021b), but is also necessary for coal mining under buildings, railways, and water bodies and the practice of sound environmental governance in mines.

2. General situation in the mine and at its working faces

For Xinji No. 2 coal mine in Huainan city, the working face 210108 in the upper slice of the coal seam #1 and the working face 210107 in the lower slice is being mined. Located in the mining area 2101 in the east wing of the coal seam #1 in the second level in Xinji coal mine, the elevations of upper and lower limits separately are -601.2 m and -648.5 m in the backstoping working face. The distance to the belt transporter tunnel of the working face 210108 in the north is about 5 m, the overlying working face 210108 in the coal seam #1upper had been mined out in December 2013, and open-off cut of the working face 210107 is staggered outwards for 10 m relative to that of the working face 210108. Within the working face, the coal seam #1 is 0 to 1.6 m (average, 1.0 m) from the overlaying coal seam (coal seam #1upper used hereafter) (basically mined out), while the distance from the underlying Taiyuan formation 1 is 15.7 m to 19.4 m (average, 17.2 m).

An analysis was performed according to geological data revealed by the mining of the working face 210108, as well as the air way, the belt transporter tunnel, and the open-off cut of working face 210107. The layout of mining area 21010 is shown in Fig. 1.

Coal seam #1 is dominated by powdery coal and is

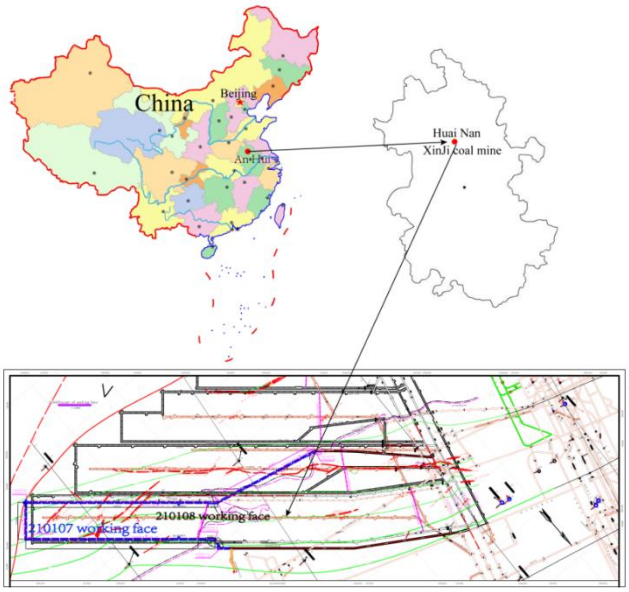

Fig. 1 Layout of mining area 21010

mainly composed of semi-bright coal with a simple structure. The roof close to the coal seam mainly contains argillaceous inclusions, while the floor shows sand-shale interbedding. The average thickness of the roof and floor changes from 1 m to 3 m. The roof of the working face 210108 had caved and collapsed, and formed a regenerated roof under the effects of its geology.

3. Theoretical analysis of ground stress behavior under a regenerated roof

Under the special geological conditions of this regenerated roof, the movement of the roof and floor is complex and mine stress are distributed in a non-uniform manner, so that coal and rock dynamic disasters readily occur. To study ground stress behavior, we established a mechanical model of an elastic thin plate for the roof of the lower slice for calculation purposes, aiming to obtain a deflection equation of the roof of the lower slice after mining and to set critical conditions for avoiding fracturing under the regenerated roof.

3.1 Theory of the elastic thin plate

In the theory of an elastic thin plate, a plate with much thickness h much less than its length and known width is defined as an elastic thin plate. In accordance with Kirchhoff's theory (Bacciocchi *et al.* 2020), the basic assumptions for the elastic thin plate include:

(1) Before deformation, a straight line perpendicular to the middle plane remains perpendicular to the deformed middle plane and the length is unchanged, that is, the assumption of straight line in the theory of plates and shells.

(2) Points in the middle plane of the plate do not show displacement parallel to the plane.

(3) Strain caused by normal stress δ_z perpendicular to mid-plane of the thin plate is ε_z=0.

The bending moment and torque equations of the thin plate are:

$$M_x=-D\left(\frac{\partial^2 w}{\partial x^2}+\mu\frac{\partial^2 w}{\partial y^2}\right),\quad M_y=-D\left(\frac{\partial^2 w}{\partial y^2}+\mu\frac{\partial^2 w}{\partial x^2}\right),\quad M_{xy}=-D(1-\mu)\frac{\partial^2 w}{\partial x\partial y} \tag{1}$$

where, D represents the flexural rigidity of the plate and D= $\frac{Eh^3}{12(1-\mu^2)}$. E and μ indicate the elastic modulus and Poisson's ratio of the plate, respectively.

The plane stress component of the plate is shown as:

$$\sigma_x=\frac{12M_x z}{h^3},\quad \sigma_y=\frac{12M_y z}{h^3},\quad \tau_{xy}=\frac{12M_{xy} z}{h^3} \tag{2}$$

Suppose that the plate is located on a continuous elastic foundation and bent by load $q(x,y)$ perpendicular to the plate. When the deflection is much less than the thickness of the plate, the sub-grade reaction R at any point of the plate is directly proportional to the deflection of the plate at this point according to Winkler's assumption, that is,

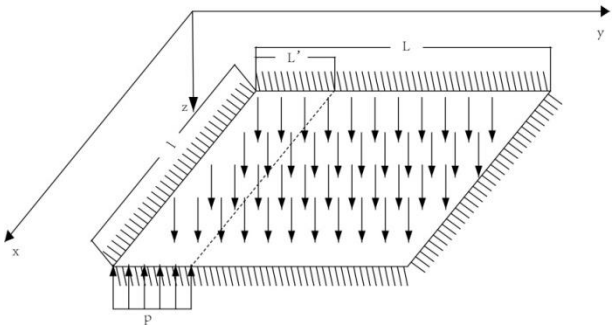

Fig. 2 Model of a rectangular cantilever plate

$$R=kw \tag{3}$$

where k is the elastic foundation coefficient, so the strength of each point acting on the plate is

$$Q=q(x,y)-kw \tag{4}$$

Therefore, the differential equations for curved surface of the elastic foundation plate can be obtained as follows:

$$D\left(\frac{\partial^4 w}{\partial x^4}+2\frac{\partial^4 w}{\partial x^2\partial y^2}+\frac{\partial^4 w}{\partial y^4}\right)=q(x,y)-kw \tag{5}$$

3.2 Establishment of model of rectangular cantilever plate under a regenerated roof

At working face 210107 in the Xinji No. 2 coal mine, the length of the working face is about 130 m and the advancing length is about 600 m. Moreover, the layer thickness of main roof in overlying strata is 1.1 m on average. According to the theory of an elastic thin plate (Bacciocchi *et al.* 2020), the ratio of thickness *h* to width *a* is about 1/110, so it can be regarded as thin.

Assuming that the hydraulic supports can ensure that the main roof is not fractured, then the main roof can be considered as an elastic thin plate with a fixed side and three free sides. The load from overlying strata on the top can be equivalent to a uniformly-distributed load *q*, and the working resistance of the front hydraulic support can be simplified as uniformly-distributed force *p*. Due to the large size of the plate, the other parts are considered unconstrained. Therefore, in view of the roadway and roof after mining, it can be modelled as a rectangular cantilever thin plate with the upper part bearing load from overlying strata while the lower part has a fixed side and three free sides supported by hydraulic supports (Fig. 2).

Taking an inner-corner of the plate as the origin, the coordinate system is established along the advance direction of the working face as the y-axis and the direction along length of the working face as the x-axis (Fig. 2). Where, l, *L*, *L'*, q and p indicate the length of the working face, advancing length of the working face, the roof-control distance of the coal mining face, the uniformly distributed load from overlying strata and the support strength of

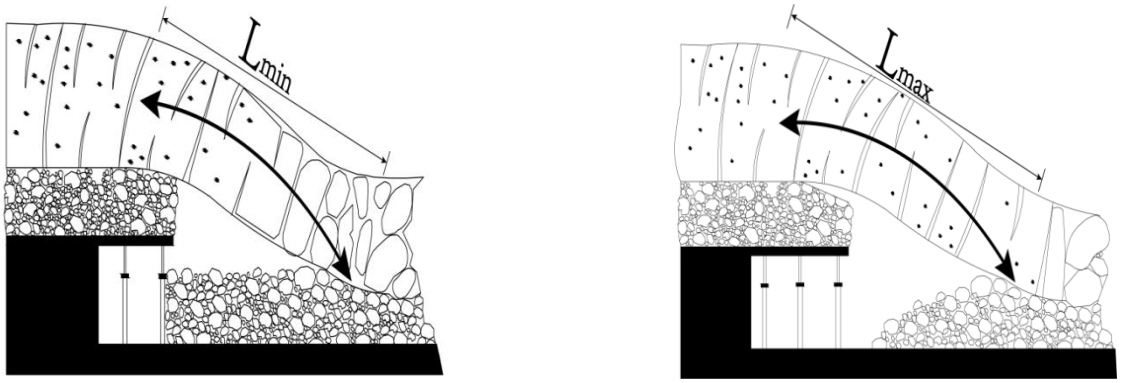

(a) (b)

Fig. 3 Arcuate structural model of the regenerated roof: (a) Before instability and (b) After instability

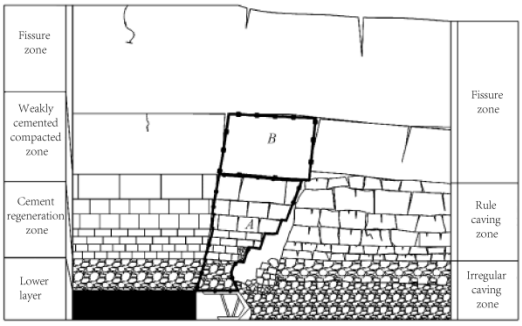

Fig. 4 Distribution of each zone in the regenerated roof

hydraulic supports, respectively.

3.3 Establishment of the improved model with an arcuate structure

In fact, the real data pertaining to thickness and load on the immediate roof of working face 210107 (the lower slice) were not detected before mining. This is because the roof of the working face 210108 (the upper slice) in Xinji No. 2 coal mine caved during mining and was re-compacted and bonded into the roof of the lower slice after a period under stratal stress due to bondability of rock or addition of water and binder. At present, it is thought that we should consider the structure of the regenerated roof as an arch in equilibrium after the roof collapses, thus stabilising the roof and a new roof is formed due to compaction and cementation in later stage (Lomax *et al.* 2019, Xue *et al.* 2020). The better to analyse the ground stress behavior under a regenerated roof, a mechanical model with an arcuate structure representing the regenerated roof was established to analyse the thickness of the regenerated roof in combination with the above model of the rectangular cantilever plate, as shown in Fig. 3.

For the regenerated roof with its arcuate structure, as the working face advances, the span of the arch changes from expansion, to shrinkage, and expansion again. This causes a loss of stability and weighting of the arch-like structure. Owing to the cemented layer of the regenerated roof having a low strength, poor stability, and suffering large plastic deformation, the damaged rock blocks on the roof cover the cemented layer in the form of an arcuate structure. Although

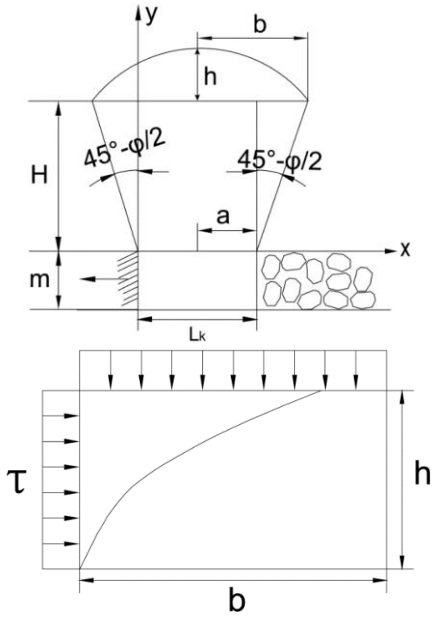

Fig. 5 Analytical model of the regenerated roof

the periodic instability found therein can result in the increase of the working face weighting, because of small damaged rock blocks therein, the maximum span L_{max} leading to instability of the arcuate structure is small. In addition, the plastic buffering effect of the underlying cemented layer results in negligible weighting when instability occurs, a small step distance, and a low intensity failure. Therefore, the thickness of cemented layer of the regenerated roof is an important factor influencing the stability of the regenerated roof. Therefore, the approximate minimum thickness of any required cemented layer is calculated by using soil mechanics theories based on known structural characteristics of the regenerated roof. The specific mechanical model is shown in Figs. 4 and 5.

Supposing that the regenerated roof is well formed, both sides of the roof-control area are compacted walls, and in case of a small caving height, when the load-reducing arch is in equilibrium, the thickness of the cemented layer is determined by the maximum shear stress τ_{max}. In other words, taking the derivative of the general b value of the span of the arch with respect to τ and setting it to 0, the minimum thickness h_{min} of the cemented layer is obtained

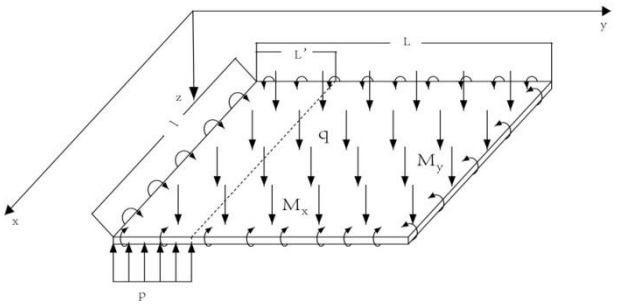

Fig. 6 The simplified mechanical model of the rectangular cantilever plate

as follows:

$$h_{\min} = K \cdot \frac{b'}{2\tan\varphi} \tag{6}$$

where, K represents the correction coefficient and is selected according to different coal and strata parameters; φ indicates the internal friction angle and values φ = 37° based on the optimum moisture content (7%); b' is the unsupported roof distance, namely, a+b and generally a = 0.2 m; and b denotes the row spacing of working face supports (m).

3.4 Comprehensive analysis of the structural model of the regenerated roof and simplified model of the elastic rectangular cantilever thin plate

Based on the above analysis, by using the principle of equivalent replacement (Lydzba *et al*. 2019), this model of a rectangular cantilever thin plate is simplified to a model of a plate with thickness $h_{\min}$, one simply supported side and thee free sides. Each side is affected by bending moments $M(x)$ and $M(y)$. The bending moment $M(x)$ is distributed on both sides y = 0 and y = l and changes with location x of a point. The bending moment $M(y)$ acts on both sides x = 0 and x = L and varies with location y of a point. The simplified model is displayed in Fig. 6.

When the rectangular cantilever plate bears load on its free sides, the boundary and corner conditions are as follows:

$$(w)_{y=0} = 0, (M_y)_{y=L} = 0, (M_x)_{x=0} = 0, (M_x)_{x=l} = 0 \tag{7}$$

$$(\frac{\partial w}{\partial y})_{y=0} = 0, (V_y)_{y=L} = f(x), (V_x)_{x=0} = 0 \tag{8}$$

$$\begin{cases} w_{(0,0)}=0, w_{(l,0)}=0, M_{y(0,L)}=0, M_{y(l,L)}=0 \\ M_{x(0,0)}=0, M_{x(l,0)}=0, M_{x(0,l)}=0, M_{x(l,L)}=0 \end{cases} \tag{9}$$

$$\frac{\partial w}{\partial y}_{(0,0)} = 0, \frac{\partial w}{\partial y}_{(l,0)} = 0 \tag{10}$$

$$R_{(0,L)} = 0, R_{(l,L)} = 0 \tag{11}$$

In accordance with the generally used methods for solving plate problems in mechanics, the double sine series proposed by Navier can be selected as the governing equation describing the curved plane of the plate:

$$w = \sum_m \sum_n A_{mn} \sin\alpha x \sin\beta y \tag{12}$$

where, $A_{mn} = \dfrac{4\int_l^0 \int_0^L q \sin\alpha x \sin\beta y dx dy}{DLl(L^2+l^2)^2}$

Thus the general solution to Eq. (5) is:

$$\begin{aligned} w = &\sum_m [A_m sh\alpha(L-y) + B_m sh\alpha y + C_m \alpha y ch\alpha(L-y) + D_m \alpha y ch\alpha y] \sin\alpha x / \sin\alpha L \\ &+ \sum_n [E_n sh\beta(l-x) + F_n sh\beta x + G_n \beta x ch\beta(l-x) + H_n \beta x ch\beta x] \sin\beta y / \sin\beta l \\ &+ a_{00} + a_{10}\frac{x}{l} + a_{01}\frac{y}{L} + a_{11}\frac{xy}{lL} + a_{20}\frac{x^2}{l^2} + a_{02}\frac{y^2}{L^2} + a_{21}\frac{x^2 y}{l^2 L} + a_{12}\frac{y^2 x}{L^2 l} + a_{30}\frac{x^3}{l^3} \\ &+ a_{03}\frac{y^3}{L^3} + a_{31}\frac{x^3 y}{l^3 L} + a_{13}\frac{y^3 x}{L^3 l} + \sum_m A_{mn} \sin\alpha x \sin\beta y \end{aligned} \tag{13}$$

Based on formulae (9) and (13), (7) and (10), as well as (8) and (11), the deflection of the free sides and bending moment of the fixed side of the rectangular cantilever plate are separately given by:

$$\begin{aligned} (w)_{y=L} = &-\frac{2}{1-\mu}\sum_m D_m \sin\alpha x \\ &-\frac{2}{1-\mu}\sum_n G_n n\pi + \frac{2}{3}a_{02} + [\frac{2}{1-\mu}\sum_n (G_n + H_n) n\pi + \frac{2}{3}a_{12})\frac{x}{l} \end{aligned} \tag{14}$$

$$\begin{aligned} (M_y)_{y=0} = -D\{&\sum_m \{C_m 2\alpha^2 + [a_{02}(1-\cos m\pi) \\ &- a_{12}\cos m\pi]\frac{24\mu(1-\mu)}{m\pi L^2}\}\sin\alpha x - (a_{02} + a_{12}\frac{x}{l})\frac{2(1-\mu^2)}{L^2}\} \end{aligned} \tag{15}$$

By combining this with Formula (13), the equation for the maximum tensile stress on the regenerated roof can be obtained:

$$\sigma_{y\max} = \frac{6M_y}{h^2}, \quad \sigma_{x\max} = \frac{6M_x}{h^2} \tag{16}$$

When the stress in Eq. (15) is less than, or equal to, $[\sigma_t]$, the roof does not fracture.

It is extremely difficult to solve the plate problem and it is difficult to obtain Fourier coefficients by using a successive approximation method. For these reasons, the first two terms of the Fourier coefficient representing the bending moment of the fixed side during calculation are selected and MATLAB™ software is used to obtain a solution. The relationships between the maximum tensile stress with advancing length and thickness of the regenerated roof are obtained based on data from the Xinji No. 2 coal mine (D=0.5, C_m=C_1+C_2, a_{02}=0.5, a_{012}=0.5, α=pi/4, a_{02}=0.5, a_{012}=0.5, μ=0.3 are known or can be calculated) (Lazopoulos 2009). On this basis, the following Eq. (17) and curve (Fig. 7) are obtained:

$$\sigma = \frac{\frac{10.095}{L^2} + 3.701}{h_{\min}^2} \tag{17}$$

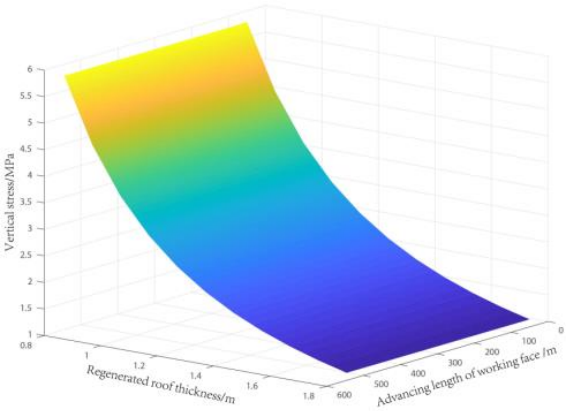

Fig. 7 Influences of thickness of the regenerated roof on vertical stress during mining

As shown in Fig. 7, as the working face advances, the vertical stress on the roof changes, that is, it increases in the initial stage, then shows a sharp decrease followed by stable decrease, and finally stabilises (This is reflected by the colour darkening from left to right in the figure and then becoming stable), however, with the reduction of thickness of the regenerated roof, vertical stress from overlying strata rises and the thinner the roof, the greater the stress increase. Based on a comparison in the figure, the effects of thickness of the regenerated roof are far greater than those of advancement of the working face. The vertical stress changes about three-fold and its maximum value is about 6 MPa, therefore, the main factor influencing stress changes in coal and strata can be determined as the thickness of the regenerated roof. To ensure safety when mining the lower slice (as far as possible), the stability after slicing the upper slice should be of paramount concern. When the thickness of the regenerated roof is set, it is important to study the changes in mine stress during mining process.

4. Numerical simulation

4.1 Introduction to software

FLAC-3D uses the explicit finite difference method and the basis of the algorithm is the fast Lagrangian calculation method. This method is most suitable for solving non-linear large-deformation problems. FLAC-3D solves the governing differential equations of a field and applies a discrete model of mixed elements, so it can simulate the yield, plastic flow, softening and large deformation of materials (Parmar *et al.* 2019).

The use of automatic inertia and automatic damping coefficient can overcome limits of a small time step and damping problem that exist in explicit formula. Furthermore, it provides interface or simulation elements known as slip-planes to simulate weak surfaces, such as faults, bedding planes, joints, and friction contact surfaces. Meanwhile, FLAC-3D also offers structural simulation elements to simulate support structural bodies, such as roadway linings, pile linings, anchor rods, and piled foundations.

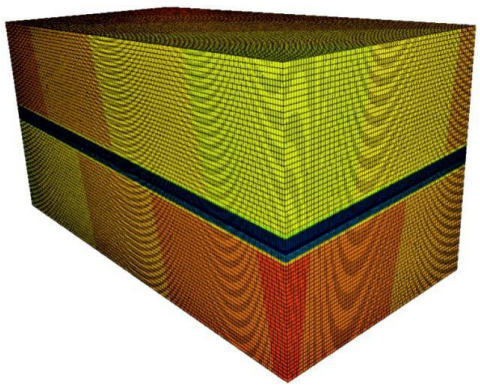

Fig. 8 Model of the mining area in Xinji No. 2 coal mine

Table 1 Physical parameters of each coal stratum

Coal and strata	Bulk modulus / GPa	Shear modulus/ GPa	Internal friction angle/ °	Tensile strength / kN	Cohesion / MPa
Upper strata	10.83e9	8.13e9	38	2.75e6	1.84e6
Roof	2.91e9	1.5e9	32	7.8e6	4e6
Coal seam #1upper	0.63e9	0.145e9	30	0.34e6	0.12e6
Coal seam #1lower	0.63e9	0.145e9	30	0.34e6	0.12e6
Floor	6.27e9	5.19e9	44.5	11.5e6	6.5e6
Lower strata	10.83e9	8.13e9	38	2.75e6	1.84e6

4.2 Model establishment

Based on prevailing geological conditions in coal seam #1 in the Xinji No. 2 coal mine, the FLAC-3D numerical simulation software was used to simulate and analyse distributions of mine stress and deformation of coal and rock in the presence of the regenerated roof. The geometric model measured 500 m × 300 m × 400 m and downhill mining was simulated on the working face. Moreover, the inclination angle of the coal and rock was 4°. The model is shown in Fig. 8.

In this model, the working face 210107 was taken as a research object. Model parameters, and layout of roadways and working faces are demonstrated in the figure. Working face 210107 measuring 390 m × 120 m with thickness of 3.6 m, and a burial depth of 800 m, is used to simulate the equivalent gravitational force of the coal and rock. According to the actual situation of the coal mine, working face 210108 should be mined first, so that the roof of the working face caves after mining, and crushed blocks and binder are subjected to high stresses to form a body acting as the roof to working face 210107. To obtain the distribution of mine stress in the presence of the regenerated roof of working face 210107, reasonable boundary conditions are selected for numerical simulation. The horizontal displacement of four vertical planes on the model is constrained in the normal direction and the bottom of the model is subjected to fixed constraints. On the top of the model, a vertical stress ($P = \gamma H$) of 23 MPa is used to simulate the weight of the covering layer. In accordance with in situ stress data collected in Xinji No. 2 coal mine, stress coefficients in x and y-directions are set to 1. An

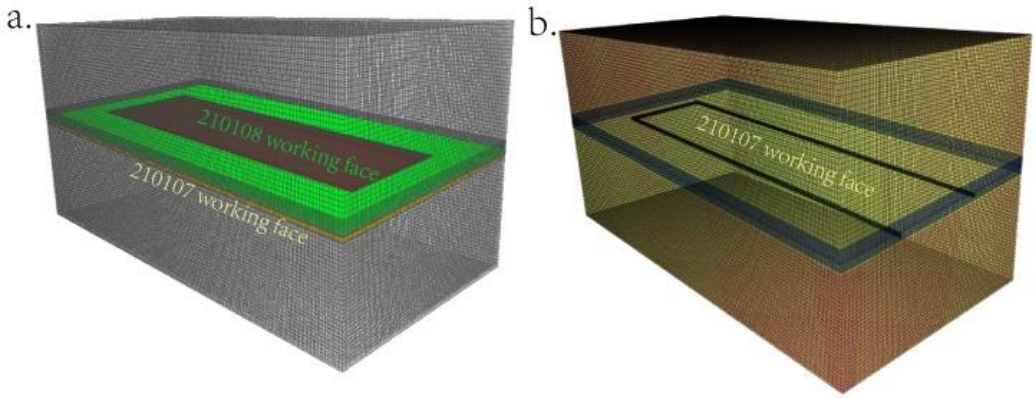

Fig. 9 Simulation of formation of the regenerated roof: (a) FLAC-3D model of working faces 210107 and 210108 and (b) Layout of working face 210107 before mining

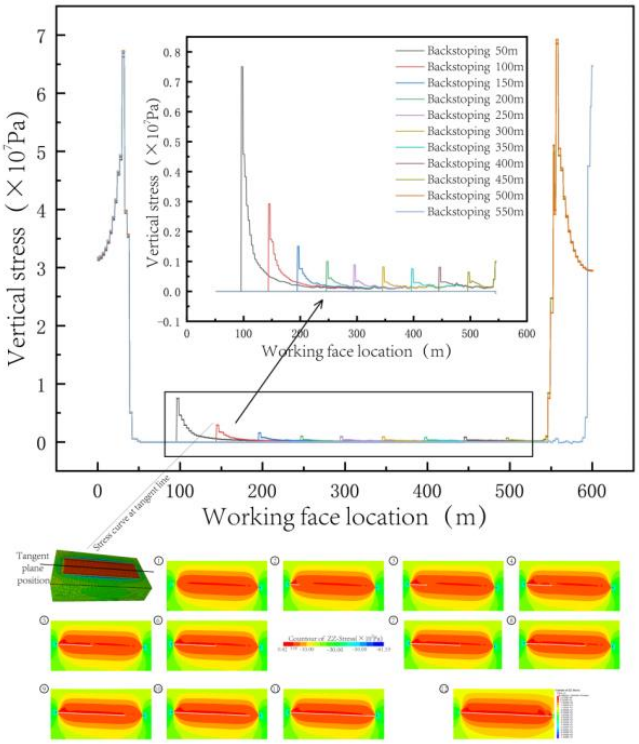

Fig. 10 Distribution of mine stress during backstoping

elasto-plastic Mohr-Coulomb model with a non-associated flow rule is selected as a failure criterion for modelling the coal as well as the roof and floor strata. Physical parameters of each coal stratum in the model are presented in Table 1.

To reflect operational mining reality as far as possible, goaf of the working face 210108 was first simulated (Fig. 9(a)), and then goaf of the working face 210108 was backfilled according to the geological parameters of the regenerated roof of working face 210107, reaching an equilibrium state (Fig. 9(b)). Finally, working face 210107 was mined. Therefore, the distribution of mine stress under the regenerated roof was obtained.

4.3 Stress evolution in the regenerated roof during backstoping

The stress change in stope is generally the forerunner of dynamic disasters, and the evolution and final distribution of stress exert different triggering effects on coal-rock impacts on working faces. Therefore, the distribution of mine stress was studied and simulated results were analysed. Moreover, the stresses in each backstoping process were plotted (Fig. 10). In this way, the influence range and magnitude of stress of overlying strata movement can be quantified, thus providing bases for disaster assessment and disaster control research.

Based on analysis of the data in Fig. 10, after backstoping of the working face, stresses in the coal and rock are released, so that stress accumulates in both ends of the goaf. At this time, the peak stress is about 70 MPa and concentration coefficient reaches about 2.8. The distribution of advance support stress on the working face first increases, decreases, and finally stabilises. The stress

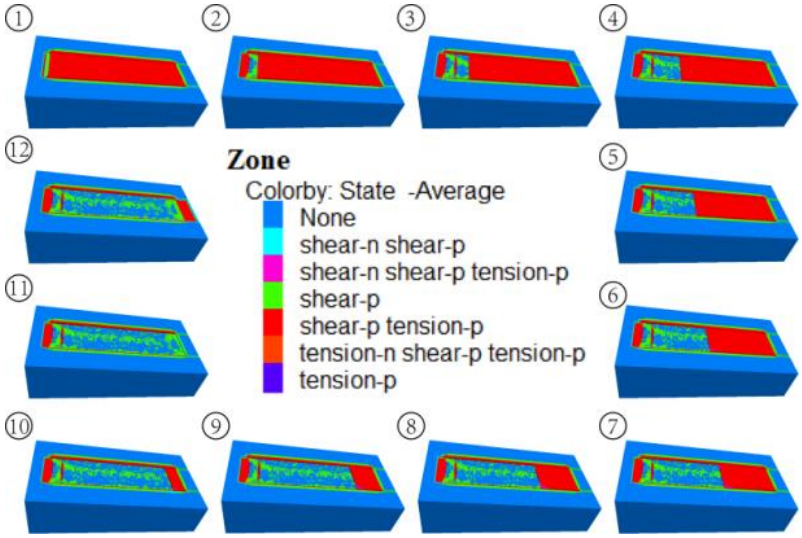

Fig. 11 Changes in plastic zone in the lower slice

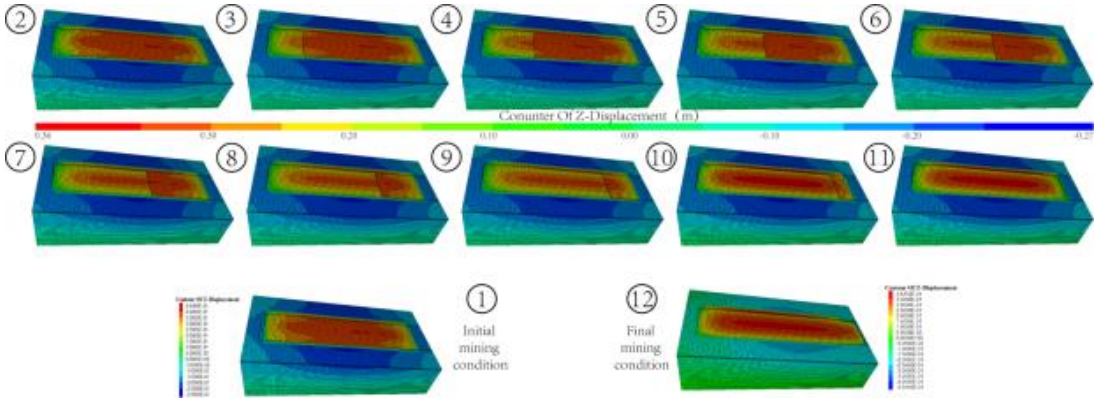

Fig. 12 Cloud pictures of displacement changes in the lower slice

concentration is generally 50 m to 100 m across and peak is generally within 20 m to 40 m in front of the working face. This area gradually decreases as the working face advances. Meanwhile, with the constantly advancing working face, peak stress gradually decreases to stable values, while several fluctuations of peak stress are found in local mining processes because periodic weighting of the mine results in periodic increase in peak stress (Meggiolaro *et al.* 2016, Meneghetti and Campagnolo 2020).

4.4 Displacement evolution in the regenerated roof during backstoping

Overlying stratal movement is an essential reason for stress changes in the stope and the occurrence of dynamic disasters. In mining, based on the physical properties of coal and rock, roof hanging structures can be easily formed and complex overlying stratal structures can be formed with coal-rock masses in stope. For this reason, when a roof hanging structure of overlying strata reaches a certain scale, or a limiting span, and bearing capacities are exceeded, roof strata fracture, thus inducing mine earthquakes through instability and movement. To analyze overlying strata movement of the mine, the cloud pictures for the changes in plastic zone and displacement of the working face in the lower slice were obtained through simulation and analysis (Fig. 11).

According to these cloud pictures, the working face is subjected to damage caused by shear stress and tensile stress in the initial stages of mining, while the area of shear failure is smaller than that of tensile failure. At this time, caving and collapse of the regenerated roof mainly results from roof caving caused by tensile failure of the surrounding rocks, and correspondingly roof displacement reduces slightly. As the working face constantly advances, it is shearing action that mainly causes the failure of the regenerated roof. While mining the corner of the working face, there are many types of force and stress there that are higher than in other locations, so it is most likely to suffer roof caving. As shown in Fig. 11, when mining to the junction with the zone of influence of working face 210108, backstoping is mainly subjected to shear failure, because of the staggered location of the upper and lower slices at the junction resulting in a non-uniform stress distribution. Therefore, roadway support in the lower slice should be strengthened to maintain roof stability, especially at the staggered location of the upper and lower slices (Mahdevari *et al.* 2021, Najafi *et al.* 2011).

As the working face constantly advances, the displacement of the regenerated roof gradually increases

and finally stabilises. Due to deviation of the locations of the upper and lower slices, displacement on both sides of the roadway exceeds that in coal and rock. It can be seen from displacement cloud pictures (Figure 12) that displacement of the lower slice first rises, then reduces, and finally stabilises from the roadway to the deeper areas of coal and rock strata. The change evinced by the cloud pictures demonstrates that the maximum deformation appears in the centre of the goaf. It can be observed that the roof of the working face changes from V-shaped to U-shaped, showing a saddle-like shape overall. This indicates that advancement of the working face significantly affects the rebalance of mine stress.

During mining, the floor heaves to form an arch shape. After mining, floor heave-induced displacement presents an elliptical distribution, and the heave increases from the middle of the working face to the four sides within 0.05 m to 0.3 m, mainly showing hemispherical variations in space. The reason is as follows: because of the constant advancement of the working face, continuous accumulation of stope length damages coal and rock and the maximum subsidence caused by backstoping of the working face gradually increases. When the cumulative length of the mining area reaches a point where the area is sufficiently mined, the maximum subsidence induced by backstoping of the working face reaches a maximum and stabilises.

5. Evolution of mining-induced stress under a regenerated roof

By mainly observing the range of influence when mining working face 210107 on the two gate roadways, we obtained the influence range and intensity of the advance support stress along the working face. On this basis, this research assessed the stress changes in front of the working face, as it was advanced, to provide guidance for determining the advance support range and strength of the working face. By observing support stress on the side of a coal pillar, the distribution of lateral abutment stress of the coal pillar was obtained. In addition, we analysed whether, or not, the setting of a coal pillar between the two working faces is reasonable and described the changes in stress on the coal pillar as the working face advanced.

5.1 Test equipment and arrangement of monitoring points

To monitor changes in mine stress, the KJ821 stress monitoring system (Fig. 13) was selected, which can monitor stress in the coal-rock mass and their distribution and evolution in real-time, provide intelligent, remote, real-time monitoring and early warning of accidents. In comparison with other methods, it has higher sensitivity, stronger anti-interference ability and reliability, which provides bases for mastering mine stress changes and preventing dynamic disasters, such as impact stress incidents. Furthermore, it can be used for monitoring stress changes in a coal-rock mass in areas affected by mining, fractured areas, and zones of high rock stress, giving early warning of coal and gas outbursts, observation of mine

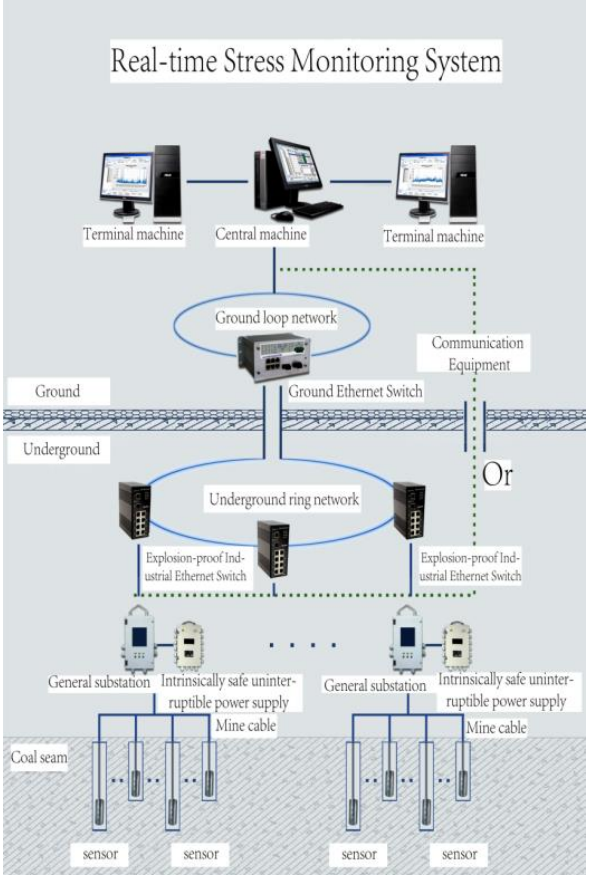

Fig. 13 The KJ821 stress monitoring system

stress, and testing broken rock zones of tunnels or roadways and assessing stress states therein.

In combination with cloud pictures showing distributions of mine stress, the main influence range of mine stress is within 15 m to 35 m to the north and 5 m to 15 m to the south of the working face. The stress reaches its peak during initial mining of the working face because there are certain regional differences between mining the upper slice and backstoping the lower slice of the working face, so that mine stress vary at the edge of the working face. It is necessary to observe the range of influence of mining activities at the working face (its lower slice) on the two gate roadways, giving the range of influence and intensity of advance support stress along the working face and assessing changes in stress in front of the working face as it advances to assist design of supporting works (Stockmann *et al.* 2013). Aiming at these, four stress monitoring points were arranged in the air-return roadway and the belt transporter tunnel some 100 m from the front of the working face in the lower slice (avoiding areas influenced by mining). Moreover, holes were drilled in the inner coal walls of the coal seam along the inclination direction of the coal seam. The diameter of the drill was 75 mm and the hole-spacing was 10 m. Holes with depths of 8 m and 15 m were separately arranged (Fig. 14).

5.2 Analysis of test results

According to the corresponding eight groups of data

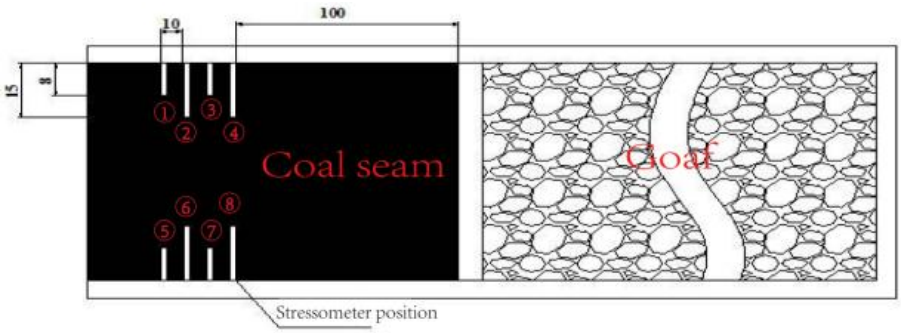

Fig. 14 Distribution of monitoring points

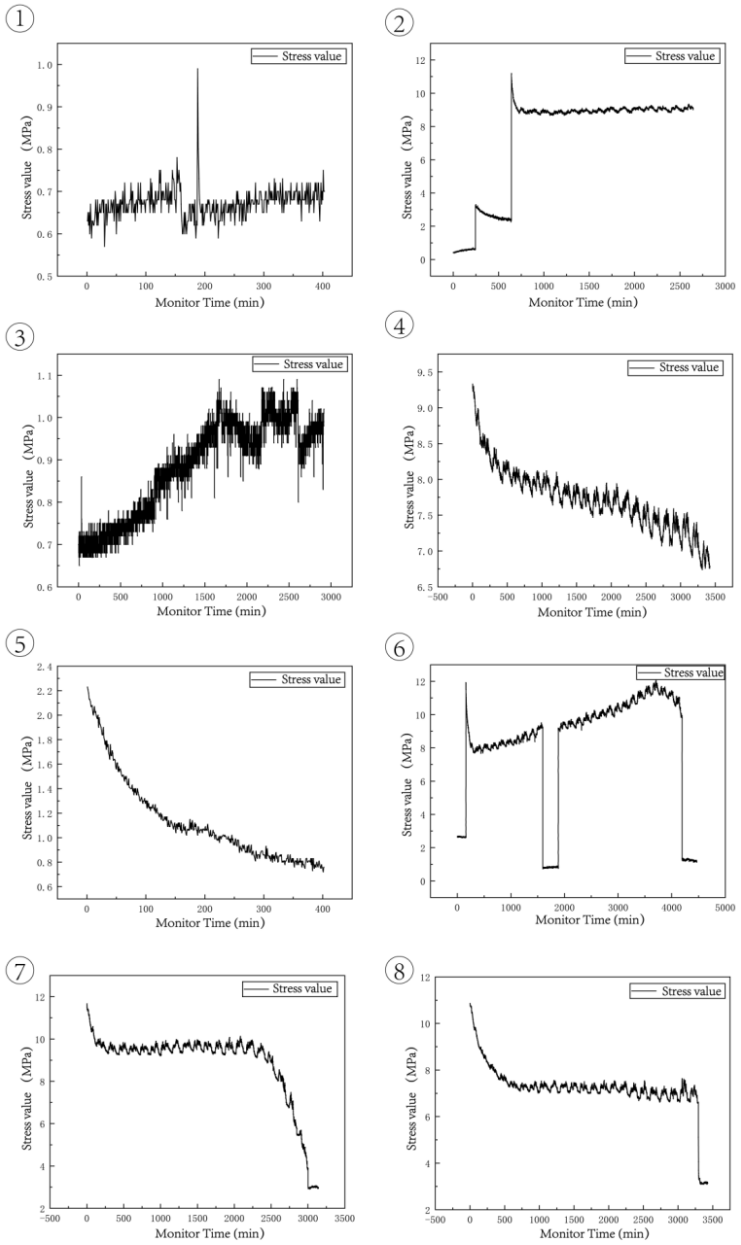

Fig. 15 Changes in mine stress during mining

obtained through field monitoring, time-stress curves were drawn (Fig. 15).

Based on the above figure, the stress in working face 210107 is distributed uniformly and changes only slightly during mining. This is because the monitoring site is 100 m from the working face. Furthermore, under the regenerated roof, dynamic loads are small, roof weighting steps are short and the roof strength is low. Besides, it can be found

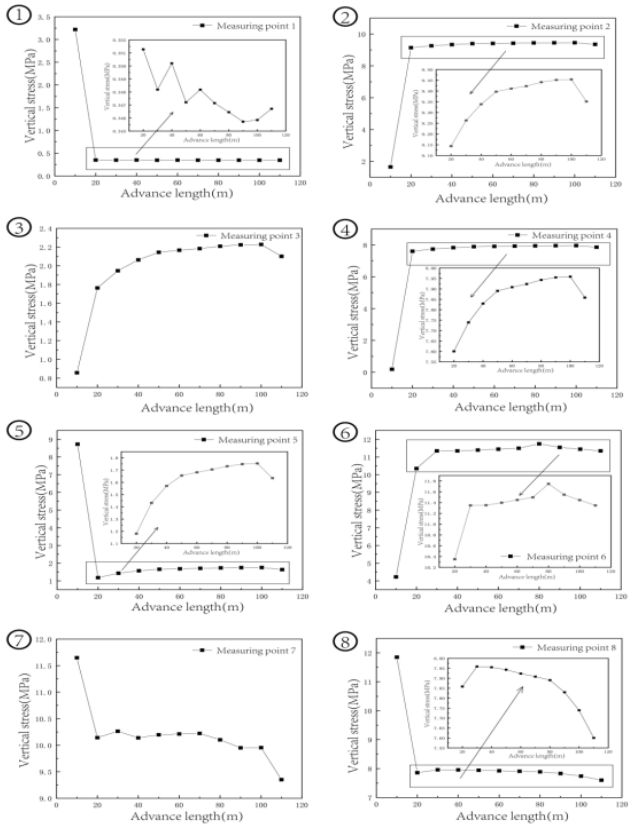

Fig. 16 Simulated stress changes at monitoring points

that mine stress mainly stabilises at between 7 MPa and 10 MPa, which is smaller than that in situ rock stress. An overall decreasing trend is shown, while mine stress at some points closer to the working face first rise and then stabilise. By analysing the simulated results, same monitoring points were simulated (Fig. 16).

By observing changes in stresses at each monitoring point, the effect distance to the working face during mining is seen. The initial stress on the working face varies in different areas. After mining for a certain period, the initial stress gradually stabilizes (Wc *et al.* 2020, Konicek *et al.* 2013), while small-amplitude fluctuations therein persist. It can be found that the stress closest to the middle of the coal seam remains stable at between 7 MPa and 12 MPa, while the mine stress near the two side walls of the roadway ranges from 0 to 4 MPa. The mine stress in front of the working face increases progressively from two sides of the roadway to the middle of the coal seam, and the further the monitoring points are from the coal mining face, the smaller the stress thereat.

5.3 Control technology for the regenerated roof

Based on the above analysis and discussions, the main causes of accidents in the regenerated roof are the damage to the integrity of the regenerated roof and the non-uniform distribution of stress during mining, so that some areas show a marked stress concentration. Moreover, according to the stress state, accidents, such as caving or rock burst in the regenerated roof occur readily (Brunton *et al.* 2010). Therefore, the following suggestions are proposed for the management of the regenerated roof:

(1) Geological analysis of the mine. After mining and caving of the upper slice, a regenerated roof is formed. Before mining the lower slice, information relating to the regenerated roof should be gathered, so as to understand specific changes and rock properties of the regenerated roof. Furthermore, before mining, the integrity and stability of the regenerated roof should be determined as far as is possible.

(2) Support management. The regenerated roof inevitably changes during mining. For this reason, to ensure stability of the roof, effective support measures should be taken and detection of changes in surrounding rocks should be improved.

(3) Timeous stress relief. Supporting works may lead to the gradual accumulation of mine stress and eventually result in rockburst accidents. Therefore, changes in mine stress should be monitored during mining, and stress should be relieved timeously in areas experiencing stress concentration.

(4) Education about safety management. Coal mining enterprises should train their employees regularly. Coal mining enterprises should formulate a safe production system in-line with the development of other enterprises in accordance with nationally-accepted good practice and norms (Jena *et al.* 2016).

6. Conclusions

The mining of the working face in the lower slice includes two processes: fracturing of the regenerated roof of overlying strata and stress release and transfer which have a certain correlation. In terms of evolution of vertical stress in stope, by analysing the relationship between movement and transformation of the regenerated roof of overlying strata and load transfter under continuous mining, the following conclusions are drawn:

(1) Based on theoretical analysis of the regenerated roof, the thicker the regenerated roof, the greater the vertical stress applied thereto. With the advancement of the working face, the vertical stress of the roof changes, mainly showing an increasing trend in the initial stages of mining; however, on the whole, the vertical stress first rises sharply, then gradually reduces in a stable fashion, before finally stabilising.

(2) With continuous backstoping of the working face, the area of goaf constantly increases and the regenerated roof of the lower slice fractures from the bottom to the top in a layer-by-layer manner. Overlying stratal movement is the primary cause of stress changes in stope and the occurrence of dynamic disasters: the former is generally the forerunner of the latter. With the constant backstoping of the working face, the peak stress on the working face in the lower slice gradually decreases until stabilising (albeit with small-amplitude fluctuations). In addition, the advance support stress on the working face first increases and then decreases with distance from the working face.

(3) Under the special conditions prevailing in a regenerated roof, the roof has a lower strength than that of

an intact roof and it is easily fractured when backstoping the working face in the lower slice, so that weighting of the working face is frequent while the weighting strength is relatively low. To avoid these potential disasters, it is necessary to control the regenerated roof as best possible, monitor the movement of the regenerated roof, and test the properties of the surrounding rocks. Furthermore, effective support methods are expected to be taken and stress is relieved timeously.

Acknowledgments

This work is supported by the National Natural Science Foundation of China (51904167, 51474134 & 51774194 & 52004143), Research Fund of the State Key Laboratory of Coal Resources and Safe Mining, CUMT (SKLCRSM19KF008), Taishan Scholars Project, Taishan Scholar Talent Team Support Plan for Advantaged & Unique Discipline Areas, Natural Science Foundation of Chongqing, China (cstc2019jcyj-bsh0041), Postdoctoral Science Foundation Project Funded by State Key Laboratory of Coal Mine Disaster Dynamics and Control (2011DA105287-BH201903), Key R&D plan of Shandong Province (2019SDZY034-2) and China Postdoctoral Science Foundation (2020M670781). We thank anonymous reviewers for their comments and suggestions to improve the manuscripts.

References

Alehossein, H., Poulsen, B.A. (2010), "Stress analysis of longwall top coal caving", *Int. J. Rock Mech. Min. Sci.*, **47**(1), 30-41. https://doi.org/10.1016/j.ijrmms.2009.07.004.

Bacciocchi, M., Fantuzzi, N. and Ferreira, A. (2020), "Conforming and nonconforming laminated finite element Kirchhoff nanoplates in bending using strain gradient theory", *Comput. Struct.*, **239**, 106322. https://doi.org/10.1016/j.compstruc.2020.106322.

Brunton, I.D., Fraser, S.J. and Hodgkinson, J.H. (2010), "Parameters influencing full scale sublevel caving material recovery at the Ridgeway gold mine", *Int. J. Rock Mech. Min. Sci.*, **47**(4), 647-656. https://doi.org/10.1016/j.ijrmms.2009.12.011.

Cheng, W., Xie, J. and Wang, G. (2009), "Comparison of strata movement between section and slicing of top coal mining in steep and thick seams", *J. China Coal Soc.*, **34**, 478-481. https://doi.org/10.13225/j.cnki.jccs.2009.04.009.

Choi, S.O. and Lee, S.J. (2015), "Three dimensional numerical analysis of the rock cutting behavior of a disc cutter using particle flow code", *KSCE J. Civ. Eng.*, **19**(4), 1129-1138. https://doi.org/10.1007/s12205-013-0622-4.

Deng, X., Zhang, J. and Kang, T. (2016), "Strata behavior in extra-thick coal seam mining with upward slicing backfilling technology", *Int. J. Min. Sci. Technol.*, **26**, 587-592. https://doi.org/10.1016/j.ijmst.2016.05.009.

Jena, S.K., Lokhande, R.D. and Manoj, P. (2016), "Analysis of strata controll monitoring in rground coal mine for apprehension of strata movement", *Recent Adv. Rock Eng.* https://doi.org/10.2991/rare-16.2016.81.

Konicek, P., Soucek, K. and Stas, L. (2013), "Long-hole destress blasting for rockburst control during deep underground coal mining", *Int. J. Rock Mech. Min. Sci.*, **61**(7), 141-153. https://doi.org/10.1016/j.ijrmms.2013.02.001.

Kong, X.G., Li, S.G. and Wang, E.Y. (2021) "Dynamics behaviour of gas-bearing coal subjected to SHPB tests", *Compos. Struct.*, **256**, 113088. https://doi.org/10.1016/j.compstruct.2020.113088.

Latifi, M., Kharazi, M. and Ovesy, H.R. (2016), "Nonlinear dynamic response of symmetric laminated composite beams under combined in-plane and lateral loadings using full layerwise theory", *Thin-Walled Struct.*, **104**, 62-70. https://doi.org/10.1016/j.tws.2016.03.006.

Lazopoulos, K.A. (2009), "On bending of strain gradient elastic micro-plates", *Mech. Res. Commun.*, **36**, 777-783. https://doi.org/10.1016/j.mechrescom.2009.05.005.

Leniak, A., Led, E. and Mirek, K. (2020), "Detailed recognition of seismogenic structures activated during underground coal mining: A case study from Bobrek Mine, Poland", *Energies*, **13**(18), 1-16. https://doi.org/10.3390/en13184622.

Li, X.L., Cao, Z.Y. and Xu, Y.L. (2020), "Characteristics and trends of coal mine safety development", *Energy Sources Part ARecovery Util. Environ. Eff.*, 1-19. https://doi.org/10.1080/15567036.2020.1852339.

Li, X.L., Chen, S.J., Li, Z.H. and Wang, E.Y. (2021), "Rockburst mechanism in coal rock with structural surface and the microseismic (MS) and electromagnetic radiation (EMR) response", *Eng. Fail. Anal.*, **124**(6), 105396. https://doi.org/10.1016/j.engfailanal.2021.105396.

Liu, S.M., Li, X.L. and Wang, D.K. (2021), "Experimental study on temperature response of different ranks of coal to liquid nitrogen soaking", *Nat. Resour. Res.*, **32**(2), 1467-1480. https://doi.org/10.1007/s11053-020-09768-3

Lomax, D.R., Massare, J.A. and Evans, M. (2019), "New information on the skull roof of Protoichthyosaurus (Reptilia: Ichthyosauria) and intraspecific variation in some dermal skull elements" *Geol. Mag.*, **157**(4), 1-11. https://doi.org/10.1017/S0016756819001225.

Lydzba, D., Rozanski, A. and Sevostianov, I. (2019), "Principle of equivalent microstructure in micromechanics and its connection with the replacement relations. Thermal conductivity problem", *Int. J. Eng. Sci.*, **144**(11), 103126. https://doi.org/10.1016/j.ijengsci.2019.103126.

Mahdevari, S. (2021), "Prediction of tailgate stability in mechanized longwall mines using an improved support vector regression model", *Arab. J. Geosci.*, **14**(3), 216. https://doi.org/10.1007/s12517-021-06598-2.

Meggiolaro, M.A., Wu, H. and Castro, J.D. (2015), "Non-proportional hardening models for predicting mean and peak stress evolution in multiaxial fatigue using Tanaka's incremental plasticity concepts", *Int. J. Fatigue*, **82**(1), 146-157. https://doi.org/10.1016/j.ijfatigue.2015.07.027.

Meneghetti, G. and Campagnolo, A. (2020), "State-of-the-art review of peak stress method for fatigue strength assessment of welded joints", *Int. J. Fatigue*, **139**(10), 105705. https://doi.org/10.1016/j.ijfatigue.2020.105705.

Najafi, M., Jalali, S.E. and Bafghi, A. (2011), "Prediction of the confidence interval for stability analysis of chain pillars in coal mines", *Safety Sci.*, **49**(5), 651-657. https://doi.org/10.1016/j.ssci.2010.11.005.

Parmar, H., Yarahmadi Bafghi, A. and Najafi, M. (2019), "Impact of ground surface subsidence due to underground mining on surface infrastructure: the case of the Anomaly No. 12 Sechahun, Iran", *Environ Earth Sci.*, **78**, 409. https://doi.org/10.1007/s12665-019-8424-8.

Rezaei, M., Hossaini, M.F. and Majdi, A. (2015), "Determination of longwall mining-induced stress using the strain energy method", *Rock Mech. Rock Eng.*, **48**(6), 2421-2433. https://doi.org/10.1007/s00603-014-0704-8.

Singh, A.K., Singh, R. and Mandal, P.K. (2002), "Inclined slicing of a thick coal seam in ascending order-A case study", *CIM*

Bull., **95**, 124-128. https://doi.org/10.1179/000705902225002394.

Smart, B.G.D. and Haley, S.M. (1987), "Further development of the roof strata tilt concept for pack design and the estimation of stress development in a caved waste", *Min. Sci. Technol*., **5**, 121-130. https://doi.org/10.1016/S0167-9031(87)90355-0.

Stockmann, M., Hirsch, D. and Lippmann-Pipke, J. (2013), "Geochemical study of different-aged mining dump materials in the Freiberg mining district, Germany", *Environ. Earth Sci*., **68**(4), 1153-1168. https://doi.org/1153-1168.10.1007/s12665-012-1817-6.

Varela, A.A., Sandoval-Albán and Muoz, M. (2021), "Evaluation of green roof structures and substrates for Lactuca sativa L. in tropical conditions", *Urban Forestry Urban Green*, **60**(5), 127063. https://doi.org/10.1016/j.ufug.2021.127063.

Wang, S. and Wang, Z. (2013), "Analysis of separation and dislocation characteristics of layered roof in the mined-out areas", *Appl. Mech. Mater*., **6**, 256-259. https://doi.org/10.4028/www.scientific.net/AMM.256-259.75.

Cao, W., Durucan, S., Cai, W., Shi, J.Q. and Korre, A. (2020), "A physics-based probabilistic forecasting methodology for hazardous microseismicity associated with longwall coal mining", *Int. J. Coal Geol*., **232**(12), 103627. https://doi.org/10.1016/j.coal.2020.103627.

Wilson, A.H. (1983), "Stress and stability in coal ribsides and pillars: Proc 1st Conference on Ground Control in Mining, Morgantown, 27–29 July 1981, Pl-12. Publ Morgantown: West Virginia University, 1981", *Int. J. Rock Mech. Min. Sci. Geomech. Abstr*., **20**, A17. https://doi.org/10.1016/0148-9062(83)91760-6.

Xue, Y.C., Sun, W.B. and Wu, Q.S. (2020), "The influence of magmatic rock thickness on fracture and instability law of mining surrounding rock", *Geomech. Eng*., **20**(6), 547-556. https://doi.org/10.12989/gae.2020.20.6.547.

Zhang, N.B., Liu, C.Y. and Yang, P.J. (2016), "Flow of top coal and roof rock and loss of top coal in fully mechanized top coal caving mining of extra thick coal seams", *Arab. J. Geosci.*, **9**(6), 1-9. https://doi.org/10.1007/s12517-016-2493-8.

Zhang, Z.B., Liu, X.N. and Zhang, Y.H. (2021a) "Comparative study on fracture characteristics of coal and rock samples based on acoustic emission technology", *Theor. Appl. Fract. Mech*., **111**(2), 102851. https://doi.org/10.1016/j.tafmec.2020.102851.

Zhang, Z.B., Wang, E.Y. and Liu, X.N. (2021b) "Anisotropic characteristics of ultrasonic transmission velocities and stress inversion during uniaxial compression process", *J. Appl. Geophys*., **186**, 104274. https://doi.org/10.1016/j.jappgeo.2021.104274.

Zou, Q.L., Lin, B.Q. and Zheng, C.S. (2015) "Novel integrated techniques of drilling–slotting–separation-sealing for enhanced coal bed methane recovery in underground coal mines", *J. Nat. Gas Sci. Eng*., **26**, 960-973. https://doi.org/10.1016/j.jngse.2015.07.033.

Zou, Q.L., Liu, H., Jiang, Z.B. and Wu, X.A. (2021) "Gas flow laws in coal subjected to hydraulic slotting and a prediction model for its permeability-enhancing effect", *Energy Sources Part A Recovery Util. Environ. Effect*. https://doi.org/10.1080/15567036.2021.1936692.